

Identifying flagella from videomicroscopy: exploiting a conserved morphology

Benjamin J. Walker^{a,*}, Richard J. Wheeler^{b,c}

^aWolfson Centre for Mathematical Biology, Mathematical Institute, University of Oxford, Oxford, OX2 6GG, UK

^bSir William Dunn School of Pathology, University of Oxford, Oxford, OX1 3RE, UK

^cNuffield Department of Medicine, University of Oxford, Oxford, OX3 7BN, UK

Abstract

Ubiquitous in eukaryotic microorganisms, the flagellum is a well-studied and highly-functional organelle that is well-known to be responsible for motility in a variety of organisms. Pertinent to multiple areas of active scientific interest is the understanding of their substructures, mechanical regulation, and beating patterns, with the latter being of particular relevance to the investigation of motile flagellated microorganisms. Commonly necessitated in their study is the capability to image and subsequently track the movement of one or more flagella using videomicroscopy, requiring digital isolation and location of the flagellum within a sequence of frames. Such a process in general currently requires some researcher input, providing some manual estimate or reliance on an experiment-specific heuristic to correctly identify and track the motion of a flagellum. Here we present a fully-automated method of flagellum identification from videomicroscopy based on the fact that the flagella appear to be of approximately constant width when viewed with typical optics. This approximate morphological characteristic, inherent in the ultrastructure of the organelle, is conserved across many eukaryotes. We demonstrate the effectiveness of the algorithm by application to captured videomicroscopy of *Leishmania mexicana*, a parasitic monoflagellate of the family *Trypanosomatidae* and the cause of a major but neglected human disease, leishmaniasis. Both high accuracy and remarkable throughput are achieved via this unsupervised method, obtaining results comparable in quality to previous studies of closely-related species but achieved without the need for precursory measurements or the development of a specialised heuristic. Further, we process a dataset documenting a canonical microswimmer that has accessory flagellar structures, the motile human spermatozoon, thus demonstrating the applicability of the presented approach to the wider class of flagellated microorganisms, enabling in general the automated generation of digitised kinematic descriptions of flagellar beating from videomicroscopy.

Keywords: Medial axis transform, Microswimmers, Segmentation, Filament

1. Introduction

Well-studied and present across a wide range of organisms, the eukaryotic flagellum is typically a long slender organelle that is known to perform a variety of functional roles throughout nature, perhaps most notably in spermatozoa where the presence of one or more flagella can render a gamete motile (Lele et al., 2013). Despite varying in function and also in lengthscale, conserved across eukaryotic flagella is the characteristic ‘9+2’ axoneme (Manton and Clarke, 1952). Formed of a central pair of singlet microtubules surrounded by nine microtubule doublets, this cytoskeletal structure is present along the length of the flagellum. This gives the organelle a well-defined diameter, although this may be obscured or complicated by the presence of accessory flagellar structures, such as the outer dense fibres of the mammalian spermatozoon (Fawcett, 1975), or the paraflagellar rod present in the parasitic

family *Trypanosomatidae* (de Souza et al., 1980). Despite structural additions to flagella, retained in typical optical videomicroscopy of flagellated organisms is an approximately conserved flagellar width, as is exemplified in Figure 1a.

Videomicroscopy of flagella at this resolution is pertinent to the study of many microswimmers, such as the classically-investigated *Crithidia oncopelti* (Holwill and McGregor, 1974) and mammalian spermatozoon (Ishijima et al., 2002, 2006; Katz et al., 1978; Ohmuro and Ishijima, 2006; Smith et al., 2009), whether for use in examining motility or exploring the mechanics of a beating flagellum. In particular, obtaining a quantitative description of a flagellar beat constitutes a key part of and a barrier to further research, with significant human effort being dedicated to the problem. Researcher input ranges from early manual approaches akin to those of Ishijima et al. (2002) and Vernon and Woolley (2002, 2004), where flagellum tracing is done by hand using acetate overlays, to semi-automated or tailored methods (Klindt et al., 2016; Mukundan et al., 2014; Riedel-Kruse and Hilfinger, 2007; Wan et al., 2014).

*Corresponding author

Email addresses: benjamin.walker@maths.ox.ac.uk (Benjamin J. Walker), richard.wheeler@path.ox.ac.uk (Richard J. Wheeler)

The work of Wan et al. (2014) and Klindt et al. (2016) on the alga *Chlamydomonas* sees the flagellum extracted from experimentally-fixed cells using custom software, with Smith et al. (2009) utilising tuned image thresholding to ascertain the beating pattern of a spermatozoan flagellum, exploiting the high contrast between the spermatozoon body and flagellum specific to this microorganism and experimental setup. Present in each of these methods is a significant need for human input, be that in the calibration of a specialised algorithm or in the manual processing of each captured image. Thus there is scope for a fully-automated method for the identification and extraction of flagellar kinematics from videomicroscopy, and any such scheme would be of relevance to a wide scientific audience.

There are numerous semi and fully-automated methods for the digital tracking of filaments, capable of accurately describing the kinematics of even overlapping structures to sub-pixel precision, some examples being the commonly-used ‘FIESTA’ software (Ruhnow et al., 2011), the generalised linear models of Xiao et al. (2016) and the ‘active contour’ methods of Goldstein et al. (2010); Hongsheng Li et al. (2009); Xu et al. (2014). Whilst invaluable in the tracking of free filaments, such methods are less applicable to the study of a moving flagellated microswimmer, where current methods may be unable to distinguish automatically between the swimmer body and any attached flagella. In particular, Figure 1a exemplifies a case where poor image contrast between a flagellum and the rest of a cell may inhibit typical thresholding methods, with the result of a bespoke thresholding algorithm being shown in Figure 1b. Thus, a different approach is necessitated to effectively process this and similar datasets, with development being warranted in the automated identification of flagella in the context of any attached bodies.

Hence, in this paper we present a general method for the identification of flagella in preprocessed videomicroscopy, focussing in particular on the segmentation of an axonemal filament from a binary frame that includes a free-swimming non-axonemal body. We exploit a feature of the filament biology that is conserved across species, and apply the resulting automatic segmentation algorithm to a large captured dataset of free-swimming *Leishmania mexicana* promastigotes, flagellated swimmers of the family *Trypanosomatidae*. We then demonstrate the applicability of the proposed method to a spermatozoon dataset, showing multi-organism efficacy, and suggest and comment on a number of possible refinements of the automated scheme.

2. Methods

2.1. A common morphological trait

As touched upon in Section 1, the 9+2 cytoskeletal structure present across eukaryotic flagella defines

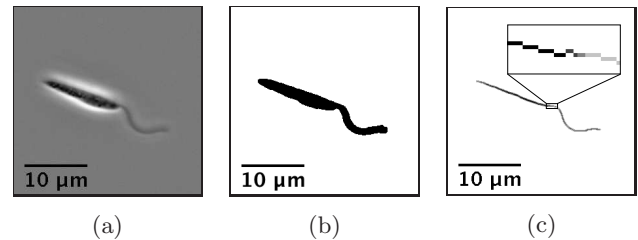


Figure 1: A sample frame taken from phase contrast videomicroscopy of a *L. mexicana* promastigote, from the dataset of Walker et al. (2018). (a) Original frame. Despite the presence of an accessory structure, the paraflagellar rod, at the recorded resolution the flagellum appears to be of approximately-constant width. (b) Result of processing (a) into a binary image, following background subtraction and noise reduction. Existing methods of filament extraction are unable to identify the flagellum in this image. (c) Result of the medial axis transform applied to (b), encoding the width of the cell along the medial line. Shown inset is an enlarged section of the transform.

the slender cylindrical morphology of the organelle (Manton and Clarke, 1952). The presence of this underlying structure along the entire length of the flagellum gives the filament a diameter that is approximately constant at typical optical resolutions, even when accessory structures are present. This is in stark contrast to what is in general the more-varied visible morphology of the cell body, as can be seen in Figure 1, an example of a *L. mexicana* promastigote with non-uniform body morphology. Thus the flagellar morphology may distinguish the slender organelle from the remainder of a cell, and hence we will aim to isolate the flagellum from videomicroscopy by identifying this feature, recognising it as a region of consistent visible width.

2.2. Medial axis transform

In order to locate regions of constant width and subsequently identify them as axonemal filaments, we compute the medial axis transform of an image already processed into a binary representation. The medial axis transform, as has been previously utilised in studying trypanosomatid morphology (Wheeler et al., 2012), may be thought of as the pixel-wise product of a distance map and a skeletonisation, with the distance map encoding at each point the shortest distance to a point not included in the binary mask.

As an example, consider the binary image shown in Figure 1b, obtained via a prefiltering and image intensity thresholding of Figure 1a, where the black region identifies the cell body and flagellum. Skeletonising the region gives a curve of the shape shown in Figure 1c, where we are choosing to skeletonise such that the skeleton of a connected region is also connected. Taking the product of the resulting curve with a distance map of the original binary image yields the grayscale image of Figure 1c, with points of greater magnitude (shown darker) corresponding to regions of greater width.

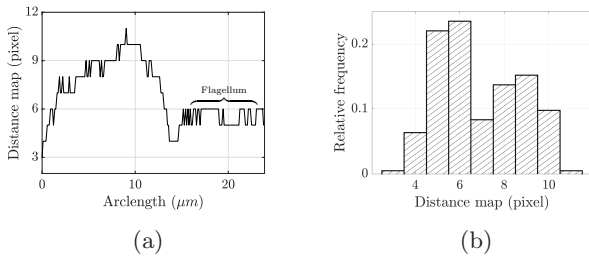


Figure 2: Analysis of a sample medial axis transform, corresponding to the cell in Figure 1. (a) Values taken by the distance map, shown in pixels, against the arclength, measured from left to right in Figure 1. The flagellum may be clearly identified from this width-profile as the segment with approximately constant width, in contrast to the varied size of the rest of the cell. (b) A histogram of the discrete values of the distance map shown in (a). A clear modal width can be seen around the flagellum width, suggesting that simple identification of the modal pixels may be sufficient to identify the flagellum in cases where the flagellar lengthscale is dominant.

2.3. Identifying the flagellar region

The results of the medial axis transform may be used to identify a region of constant width, noted in Section 2.1 to be a conserved morphological feature of flagella. Figure 2a shows an example width-profile of a flagellated swimmer, in particular the individual shown in Figure 1. With arclength being measured along the computed skeleton starting from the left-most endpoint, a region of approximately constant width can be easily identified, corresponding precisely to the flagellum. Analysis of the derivatives of this profile with respect to arclength, for example locating extrema of the first and second derivatives, can be used to isolate the point of flagellar attachment, and thus an endpoint of the flagellum, and subsequently to segment the entire flagellum by the identification of this constant-width region.

However, in many cases derivative analysis and region identification from the width-profile may be an unnecessary complication. As indicated by the histogram of Figure 2b, we note that the observed flagellar width found in Figure 2a corresponds to the approximate mode of the width distribution of the cell. As the flagellum is typically a long slender organelle, it may be reasoned to be a significant contributing factor to a mode of the width distribution, and identified as such. Thus in cases where flagellar length is relatively large it may be sufficient to simply identify those regions with cell width close to the modal value, subsequently taking care to select the largest of such regions. In particular, such modal analysis may be easily automated, and will be utilised in Section 3.

2.4. Procedure

Hence we propose that the tracing of flagella from a single frame may be achieved by the following overall procedure:

- i) pre-process into a binary mask of the entire cell;
- ii) perform and analyse a medial axis transform, isolating flagella by derivative or modal analysis;

- iii) trace the resulting isolated filaments.

Both the preprocessing and filament tracing steps may be achieved automatically by use of existing tools, for example the methods of Ruhnnow et al. (2011), Xiao et al. (2016) and Goldstein et al. (2010). The isolation of flagella via either the modal or derivative analysis suggested in Section 2.3 can also be performed without user input, with an example of a simplistic but effective automated modal analysis being provided in the Supplementary Material (Macro 1 and Macro 2).

Efficient and effective application of the above method requires datasets of suitable magnification, frame rate and contrast. In particular, magnification must be sufficiently high to clearly capture the flagella, typically with recorded flagellar width of at least $2/3$ pixels and approaching diffraction-limited magnification. Frame rates should be high enough to avoid motion blur, and contrast levels such that the organism may be readily segmented from the background.

2.5. Verification dataset

In order to verify the proposed algorithm we will process the dataset generated by Walker et al. (2018), unpublished and used with permission. Comprising of approximately 150,000 frames combined from 126 *Leishmania mexicana* promastigotes, in general the phase contrast videomicroscopy does not greatly differentiate the cell body from the attached flagellum, with the flagellum not having a different grey value to the cell body, thus existing thresholding approaches are not sufficient for the digital isolation of the flagellum.

3. Calculation

The computational procedure of Section 2.4 was implemented in the ImageJ macro language (Schneider et al., 2012). We opt in this instance to utilise the modal analysis described in Section 2.3, creating a fully automated scheme that is computationally-trivial but proves to be effective in practice. Sample macros may be found in the Supplementary Material, where image preprocessing and filament tracing have been implemented in a basic manner that is sufficient for exemplifying the flagellar identification method.

3.1. Flagellar identification in *L. mexicana*

The 150,000 frames of the dataset of Walker et al. (2018) were processed without user input using Macro 1 of the Supplementary Material, with the overall computational time (including preprocessing and filament tracing) being ca. 24 hours on a quad-core Intel® Core™ i7-6920HQ CPU running ImageJ 1.51u, with peak memory usage no more than twice the size of a single frame. To demonstrate the efficacy of the algorithm a 100-frame sample of the results is presented

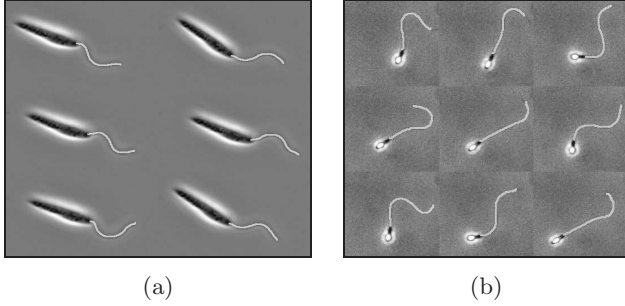


Figure 3: Composite data and results from an implementation of the proposed scheme. A montage of original frames with the identified flagella superimposed, showing very good agreement with by-eye identification, for sample (a) *L. mexicana* and (b) spermatozoa. Original frames from the datasets of Walker et al. (2018) (unpublished) and Ishimoto et al. (2017) respectively. Reprinted original frames of (b) with permission from [K. Ishimoto, H. Gad  lha, E.A. Gaffney, D.J. Smith, J. Kirkman-Brown. Physical Review Letters 118, 124501, 2017] Copyright (2017) by the American Physical Society.

in the Supplementary Material (Results 1), with the identified flagellum centreline being highlighted in white on the original sample (Dataset 1 of the Supplementary Material). In Figure 3a we showcase multiple frames of this composite as a montage, with the flagellum centreline highlighted. Clear agreement can be seen between the segmented regions and what may be identified by-eye as flagella, obtaining similar results to what may be expected of a manual-tracing method but without any researcher input. The same level of accuracy is present in an overwhelming majority of analysed frames, with any loss only occurring due to the simplistic implementation of filament tracing used here. Thus we have validated both an implementation of and the methodology behind our proposed scheme of flagellar identification, in addition to enabling a quantitative study of *L. mexicana* flagellar kinematics.

3.2. Application to a canonical flagellate

To highlight the applicability of the method and implementation to a variety of flagellated microorganisms we analyse a dataset of a swimming human spermatozoon, specifically Supplementary Movie 1 of Ishimoto et al. (2017). Example composite frames are shown in Figure 3b, and as in the case of *L. mexicana* demonstrate remarkable accuracy, but we particularly note the presence of accessory structures to the flagellum. We see that the midpiece of the flagellum has consistently not been identified, owing to the greatly-increased width in this section, whilst the principal piece is accurately segmented. However, the midpiece is itself of approximately-constant visible width, thus we hypothesise that repeated modal analysis will be able to correctly identify and even distinguish between these different sections of the flagellum, and easily adapted from the current implementation.

Processing was performed automatically using Macro 2 of the Supplementary Material, which included slight adjustments to the preprocessing of Macro 1. In this

example some sections of the flagellum briefly move out of the plane of imaging, which due to the simple preprocessing and filament tracing steps implemented here results in some errors in flagellum identification, in addition to some variations in the final traced filament length. These are easily corrected by the use of more-sophisticated approaches to these stages of computation, such as have been previously commented upon in Section 2.4.

4. Results and Discussion

In this work we have presented and verified a method of flagellar identification from the videomicroscopy of free-swimming bodies. We note the presence of a structural backbone ubiquitous in eukaryotic flagella and cilia, giving these axonemal filaments a well-defined cross-section and therefore a width. Additionally, we acknowledge that the presence of accessory structures to the axoneme may significantly alter the ultrastructure of the organelle, and therefore the width observed in videomicroscopy. However, the effects of some such structures have been considered, as for the cases of the paraflagellar rod of *Leishmania mexicana* and the outer dense fibres of particular spermatozoa, and change in visible width at typical optical resolutions and magnifications is either not significant in general or may be further exploited to identify subsections of a flagellum. Hence we proposed a procedure for the automated identification of flagella-like structures from videomicroscopy that exploited the morphological feature of consistent observed width, utilising the medial axis transform for quantification.

To extract the location of a filament from the results of the medial axis transform we have proposed two simple schemes: derivative analysis of the width-profile, where consideration of local extrema of the first and second derivatives is expected to be able to identify the proximal end of a filament, and a less-complex modal analysis of the width distribution. Having implemented and verified the latter approach, we note the scope for future work to refine the precise methodology used here by performing more-sophisticated statistical analysis, however we emphasise that even the basic scheme shown in this work was sufficient for adequate identification of filaments.

Successful identification of a flagellum here depends upon the organelle being consistently contained within the focal plane, and may be less successful in processing datasets in which large out-of-plane deviations are consistently present. The approach is also likely unsuitable for use when processing numerous cilia/flagella that may not be easily distinguished, such as those of ciliated epithelia, but is in principle readily applicable to multi-flagellated microorganisms such as *Crithidia oncopelti*.

Preprocessing and filament tracing were implemented here in a basic manner, and we recognise extensive scope for the incorporation of more-refined methods of filament segmentation, such as the ‘FIESTA’ suite

of tools and active contour methods of Ruhnnow et al. (2011) and Xiao et al. (2016) respectively, in addition to using established thresholding methods for the creation of an initial binary mask. However, despite the simplistic implementations used here, the proposed procedure was shown to provide desirable accuracy at little computational or human cost, enabling rapid quantification of flagellar motion in a sizeable dataset. Indeed, whilst the presented approach identifies flagella in individual frames, the achieved throughput is sufficiently high for use in video analysis.

A potential refinement to the proposed scheme involves combining our morphological analysis with segmentation based on signal magnitudes, valuable in cases where thresholding-based segmentation may be informative but only partially applicable. We also highlight an application to the tracking of free-swimming microorganisms, where the analysis of the width-profile may yield the location of flagellar attachment and thus enable the tracking of swimmer motion.

In summary, our proposed method for the identification of axonemal filaments has been demonstrated to be of high accuracy and able to be implemented as a fully-automated algorithm. We have verified our method on a large dataset captured of a free-swimming flagellate, and achieved a high throughput and accuracy without optimisation or refinement of a basic implementation. Notably independent of the particulars of the videomicroscopy, and reliant only on a conserved morphological feature of axonemal filaments, the considered procedure and implementations may potentially realise future study of the kinematics of a wide range of flagellated and ciliated microorganisms.

Acknowledgements

B.J.W. is supported by the UK Engineering and Physical Sciences Research Council (EPSRC), grant EP/N509711/1. R.J.W. is supported by a Wellcome Trust Sir Henry Wellcome Fellowship [103261/Z/13/Z], with equipment supported by a Wellcome Trust Investigator Award [104627/Z/14/Z].

Vitae

Benjamin J. Walker is studying towards a DPhil in Mathematics at the Wolfson Centre for Mathematical Biology, University of Oxford, having also completed his undergraduate MMATH studies in Oxford. His research interests include flagellate motion, both collective and individual, regulation of flagellar beating, and microbiological fluid dynamics.

Richard J. Wheeler is currently a postdoctoral researcher at The Sir William Dunn School of Pathology in the University of Oxford, now moving to the Nuffield Department of Medicine to set up his own research group

as a Wellcome Trust Sir Henry Dale Fellow. Topics of current research include the study of *Leishmania mexicana*, specifically regarding flagellum shape and function, along with a particular interest in automated image analysis.

References

- Fawcett, D.W., 1975. The mammalian spermatozoon. *Developmental Biology* 44, 394–436. doi:10.1016/0012-1606(75)90411-X.
- Goldstein, T., Bresson, X., Osher, S., 2010. Geometric Applications of the Split Bregman Method: Segmentation and Surface Reconstruction. *Journal of Scientific Computing* 45, 272–293. doi:10.1007/s10915-009-9331-z.
- Holwill, M.E., McGregor, J.L., 1974. Micromanipulation of the flagellum of *Crithidia oncopelti*. I. Mechanical effects. *The Journal of Experimental Biology* 60, 437–44.
- Hongsheng Li, Tian Shen, Smith, M.B., Fujiwara, I., Vavylonis, D., Xiaolei Huang, 2009. Automated actin filament segmentation, tracking and tip elongation measurements based on open active contour models, in: 2009 IEEE International Symposium on Biomedical Imaging: From Nano to Macro, IEEE. pp. 1302–1305. doi:10.1109/ISBI.2009.5193303.
- Ishijima, S., Baba, S.A., Mohri, H., Suarez, S.S., 2002. Quantitative analysis of flagellar movement in hyperactivated and acrosome-reacted golden hamster spermatozoa. *Molecular Reproduction and Development* 61, 376–384. doi:10.1002/mrd.10017.
- Ishijima, S., Mohri, H., Overstreet, J.W., Yudin, A.I., 2006. Hyperactivation of monkey spermatozoa is triggered by Ca²⁺ and completed by cAMP. *Molecular Reproduction and Development* 73, 1129–1139. doi:10.1002/mrd.20420.
- Ishimoto, K., Gadêlha, H., Gaffney, E.A., Smith, D.J., Kirkman-Brown, J., 2017. Coarse-Graining the Fluid Flow around a Human Sperm. *Physical Review Letters* 118, 124501. doi:10.1103/PhysRevLett.118.124501.
- Katz, D.F., Mills, R.N., Pritchett, T.R., 1978. The movement of human spermatozoa in cervical mucus. *Reproduction* 53, 259–265. doi:10.1530/jrf.0.0530259.
- Klindt, G.S., Ruloff, C., Wagner, C., Friedrich, B.M., 2016. Load Response of the Flagellar Beat. *Physical Review Letters* 117, 1–5. doi:10.1103/PhysRevLett.117.258101.
- Lele, P.P., Hosu, B.G., Berg, H.C., 2013. Dynamics of mechanosensing in the bacterial flagellar motor. *Proceedings of the National Academy of Sciences* 110, 11839–11844. doi:10.1073/pnas.1305885110.
- Manton, I., Clarke, B., 1952. An Electron Microscope Study of the Spermatozoid of *Sphagnum*. *Journal of Experimental Botany* 3, 265–275. URL: <http://www.jstor.org/stable/23686102>.
- Mukundan, V., Sartori, P., Geyer, V.F., Jülicher, F., Howard, J., 2014. Motor regulation results in distal forces that bend partially disintegrated *Chlamydomonas* axonemes into circular arcs. *Biophysical Journal* 106, 2434–2442. doi:10.1016/j.bpj.2014.03.046.
- Ohmuro, J., Ishijima, S., 2006. Hyperactivation is the mode conversion from constant-curvature beating to constant-frequency beating under a constant rate of microtubule sliding. *Molecular Reproduction and Development* 73, 1412–1421. doi:10.1002/mrd.20521.
- Riedel-Kruse, I.H., Hilfinger, A., 2007. How molecular motors shape the flagellar beat. *HFSP Journal* 1, 192–208. doi:10.2976/1.2773861.
- Ruhnnow, F., Zwicker, D., Diez, S., 2011. Tracking Single Particles and Elongated Filaments with Nanometer Precision. *Biophysical Journal* 100, 2820–2828. doi:10.1016/j.bpj.2011.04.023.
- Schneider, C.A., Rasband, W.S., Eliceiri, K.W., 2012. NIH Image to ImageJ: 25 years of image analysis. *Nature Methods* 9, 671–5. URL: <http://www.ncbi.nlm.nih.gov/pubmed/22930834>.
- Smith, D.J., Gaffney, E.A., Gadêlha, H., Kapur, N., Kirkman-Brown, J.C., 2009. Bend propagation in the flagella of migrating

- human sperm, and its modulation by viscosity. *Cell Motility and the Cytoskeleton* 66, 220–236. doi:10.1002/cm.20345.
- de Souza, W., Souto-Pradón, T., Souto-Pradon, T., 1980. The Paraxial Structure of the Flagellum of Trypanosomatidae. *The Journal of Parasitology* 66, 229. doi:10.2307/3280809.
- Vernon, G.G., Woolley, D.M., 2002. Microtubule displacements at the tips of living flagella. *Cell Motility and the Cytoskeleton* 52, 151–160. doi:10.1002/cm.10041.
- Vernon, G.G., Woolley, D.M., 2004. Basal sliding and the mechanics of oscillation in a mammalian sperm flagellum. *Biophysical Journal* 87, 3934–3944. doi:10.1529/biophysj.104.042648.
- Walker, B.J., Wheeler, R.J., Ishimoto, K., Gaffney, E.A., 2018. Boundary behaviours of *Leishmania mexicana*: a hydrodynamic simulation study. URL: <http://arxiv.org/abs/1806.00373>.
- Wan, K.Y., Leptos, K.C., Goldstein, R.E., 2014. Lag, lock, sync, slip: the many ‘phases’ of coupled flagella. *Journal of The Royal Society Interface* 11, 20131160–20131160. doi:10.1098/rsif.2013.1160.
- Wheeler, R.J., Gull, K., Gluenz, E., 2012. Detailed interrogation of trypanosome cell biology via differential organelle staining and automated image analysis. *BMC Biology* 10, 1. doi:10.1186/1741-7007-10-1.
- Xiao, X., Geyer, V.F., Bowne-Anderson, H., Howard, J., Sbalzarini, I.F., 2016. Automatic optimal filament segmentation with sub-pixel accuracy using generalized linear models and B-spline level-sets. *Medical Image Analysis* 32, 157–172. doi:10.1016/j.media.2016.03.007.
- Xu, T., Vavylonis, D., Huang, X., 2014. 3D actin network centerline extraction with multiple active contours. *Medical Image Analysis* 18, 272–284. doi:10.1016/j.media.2013.10.015.